

## Effect of the pH of Solutions on the Coercivity and Microstructure of Chemically Deposited CoP Films

A. V. Chzhan<sup>a, b, \*</sup>, S. A. Podorozhnyak<sup>a</sup>, M. N. Volochaev<sup>c</sup>,  
G. N. Bondarenko<sup>d</sup>, and G. S. Patrin<sup>a, c</sup>

<sup>a</sup> Siberian Federal University, Krasnoyarsk, 660041 Russia

<sup>b</sup> Krasnoyarsk State Agricultural University, 660130 Russia

<sup>c</sup> Kirensky Institute of Physics, Federal Research Center KSC SB RAS,  
Krasnoyarsk, 660036 Russia

<sup>d</sup> Institute of Chemistry and Chemical Technology, Federal Research Center KSC SB RAS,  
Krasnoyarsk, 660036 Russia

\*e-mail: avchz@mail.ru

Received December 20, 2016

**Abstract**—Specific features of the variation in the microstructure and coercivity  $H_C$  of chemically deposited CoP films with the pH of the solutions are determined. It is established that around pH  $\sim 8.5$ , the film undergoes the structural transition from the submicrocrystalline to nanocrystalline state, which is followed by the transition from the crystalline to amorphous phase. It is demonstrated that the observed transition is not accompanied by the change in the crystallographic structure and is caused by a decrease in the geometrical sizes due to embedding of P atoms. It is found that the CoP films fabricated at pH  $\sim 8.5$  have the properties characteristic of compact nanocrystalline materials.

DOI: 10.1134/S1063783417070058

### 1. INTRODUCTION

Thin magnetic films (TMFs) based on Co and P alloys find wide application in various designs, which is related mainly to their possible use in forming both high- and low-coercivity samples [1]. As is known, the coercivity  $H_C$  depends, to a great extent, on the crystal structure of a film. The microstructure of the CoP films fabricated by a chemical technique is significantly affected by alkaline agents (sodium hydrocarbonate or ammonia), which change the pH (potential of hydrogen) of a solution and, consequently, the relative Co and P contents in the films [2]. In this study, we report X-ray and electron diffraction data on the structural changes in the CoP films upon variation in the acidity of working solutions.

### 2. EXPERIMENTAL

The investigated films with a thickness of  $\sim 50$  nm were deposited onto glass substrates by chemical reduction of Co and P from aqueous solutions [3, 4]. The sensitizing  $\text{SnO}_2$  layer thickness was  $\sim 10$  Å and the activating Pd layer thickness was  $\sim 50$  Å. The base solution consisted of  $\text{CoSO}_4 \cdot 7\text{H}_2\text{O}$  (10 g/L),  $\text{Na}(\text{H}_2\text{PO}_2)$  (7.5) g/L, and  $\text{Na}_3\text{C}_6\text{H}_5\text{O}_7$  (25 g/L). As is known, the properties of the CoP TMFs are affected by both the pH of the reduction solution and type

(acetate, citrate, ammonium, etc.) of the complex cobalt compounds in the solution. It seems the simplest and most manufacturable to use the citrate complexes and sodium hydrocarbonate  $\text{NaHCO}_3$  or caustic soda NaOH used in this study as an alkaline agent. The required pH was specified by adding the alkali in a certain concentration. Addition of the alkali leads to the nonlinear change in the solution acidity (Fig. 1).

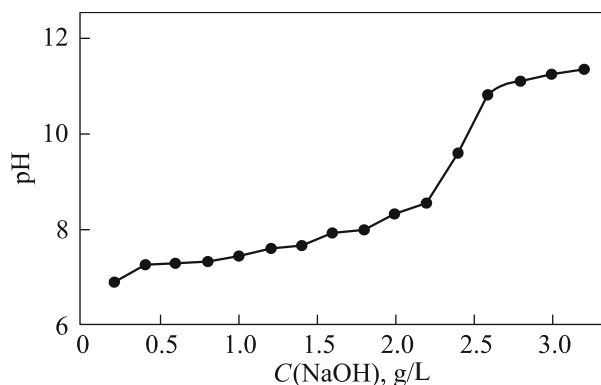


Fig. 1. Dependence of the pH of the solution on the NaOH concentration.

Composition and thickness of the films were determined by X-ray diffraction analysis (XRD) on a DRON-3 diffractometer (Cu radiation, 1.5418 Å). Film microstructure was investigated by transmission electron microscopy (TEM), including scanning transmission electron microscopy (STEM); elemental composition was studied on a Hitachi HT-7700 transmission electron microscope equipped with a Bruker X-Flash 6T/60 energy dispersive detector. For electron-microscopy investigations, the films were separated from the substrate in a weak solution of hydrofluoric acid and set onto copper grids.

### 3. RESULTS

The coercivity of the CoP films depends, to a great extent, on the pH of the working solutions used to deposit the films (Fig. 2). The increase in the pH from 7 to ~8.5 leads to the linear growth of the coercivity  $H_C$ , which attains ~900 Oe. However, with a further increase in the acidity, the  $H_C$  value drops almost stepwise to several oersteds. These features of the  $H_C$  variation reflect the structural changes observed in the CoP films upon variation in the solution acidity. In the XRD data on the samples obtained at pH < 8.5 (Fig. 3a), the high-coercivity portion corresponds to the hcp cobalt phase. The electron diffraction patterns of these samples contain textured rings characteristic of the polycrystalline structure (Fig. 3b). The almost equal heights of the fundamental peaks are indicative of the polycrystalline structure without preferred crystal growth direction.

The electron microscopy surface images (Fig. 3c) shows that the CoP film has a fine-grained structure with a grain size from 50 to 70 nm. The elemental mapping results (Fig. 4) are indicative of the almost uniform Co and P distribution in grains. It can be seen from the cross sectional image shown in Fig. 3d that there are boundary areas between neighboring grains (bright lines in the images), which separate crystallites over the entire thickness. The occurrence of such areas is related to the specific features of the liquid phase growth of the film. As was shown in [5], the film forms from islands. At the initial stage, they are isolated from each other, but, as the thickness increases, the grain size grows and only a thin spacer remains between neighboring islands. Earlier, such spacers were observed in the CoP films formed by the electrolytic method.

The transition to the low-coercivity state in the range of pH > 8.5 corresponds to the film structure change observed in the electron microscopy images (Fig. 5a). It can be seen that there are small particles inside the coarse grains whose size is comparable with the high-coercivity film crystallite size. The occurrence of the small particles is reflected well in the XRD patterns (Fig. 5b). The weak, yet unambiguously determined hcp cobalt peaks are indicative of the

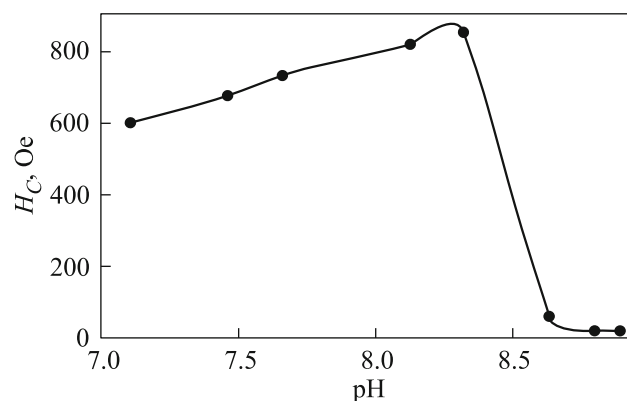


Fig. 2. Coercivity vs pH of the solution.

imperfection of the crystal lattice and nanoparticles forming it. In the electron diffraction patterns of the samples of this type, one can see the diffuse reflections (Fig. 5c) typical of nanocrystalline materials. Analysis of broadening of the diffraction lines in the electron diffraction patterns shows that the size of small particles is from 2 to 5 nm. Similar to the case of the high-coercivity CoP films, the electron microscopy images in Fig. 5a contain bright spacers separating the denser structural formations.

The elemental mapping data show that Co and P are uniformly distributed in grains, as in the case of the high-coercivity films.

According to the XRD data presented in Fig. 6b and electron diffraction pattern from Fig. 6c, with a further increase in the pH, the grains become smaller (Fig. 6a), which is accompanied by structure amorphization.

### 4. DISCUSSION

As was shown in [7], the increase in the pH leads to an increase in the P concentration and, consequently, to a decrease in the crystallite size. Based on the data obtained, we can establish that there are two regions of the pH of the chemical solutions where the regularities of the CoP film structure change with the grain size are observed. At pH < 8.5, the films are formed by microscopic and submicroscopic grains containing Co crystallites with the hcp lattice and P atoms. In this region, the change in  $H_C$  with pH is determined by the same physical mechanisms as in conventional thin ferromagnetic films. As was shown in [5], at a film thickness of no less than 10 nm, the coercivity of the CoP films is caused by the motion of domain walls (DWs); therefore, the coercivity is determined by DW pinning on inhomogeneities or by the nucleation critical field. The coercivity, which is related to the DW pinning on

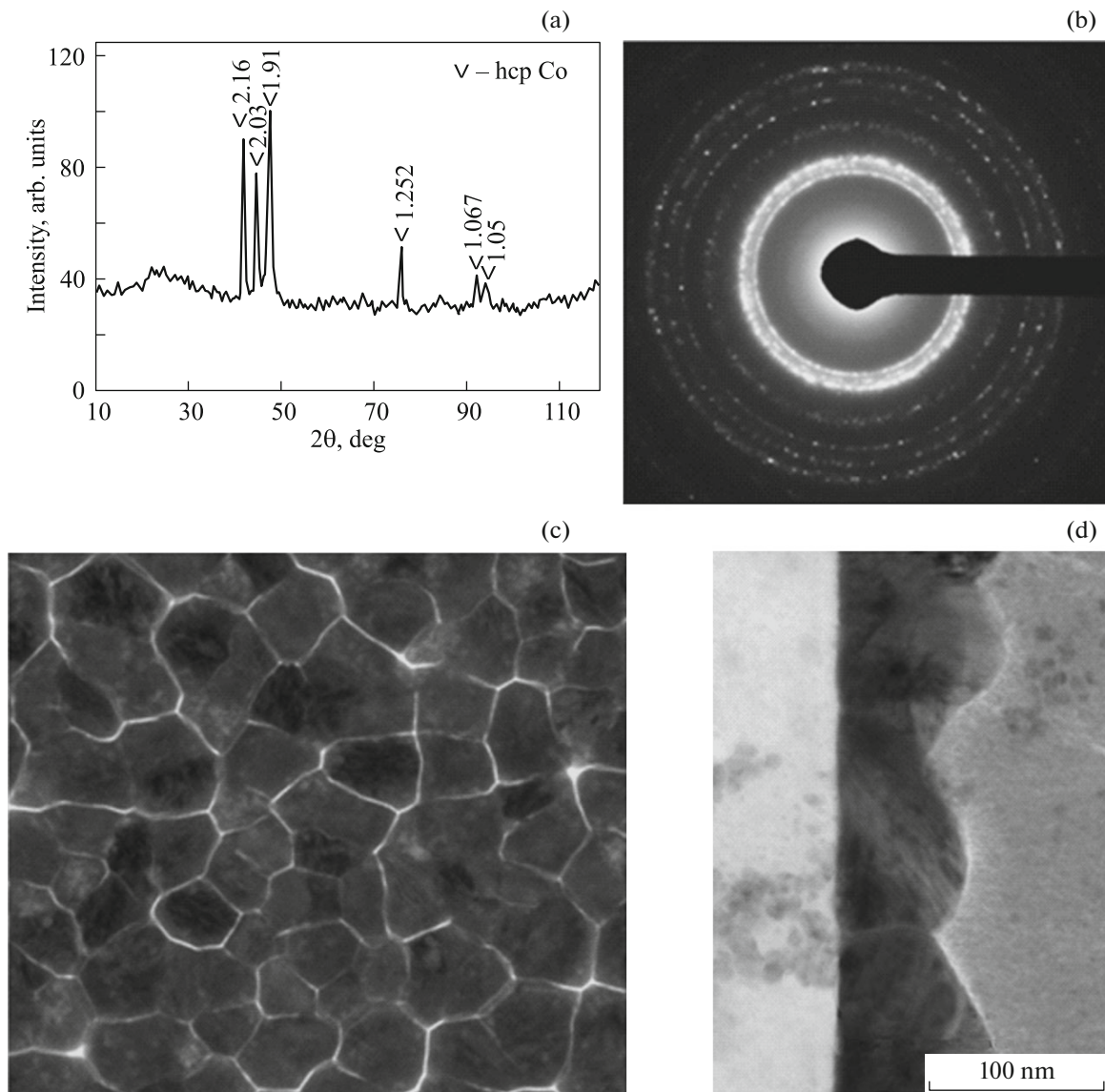


**Fig. 3.** (a) X-ray diffraction pattern, (b) electron diffraction pattern, (c) STEM image, and (d) cross section of the submicrocrystalline CoP film. Digitals above the peaks indicate interplane distances (Å) in the Co crystal lattice.

nonmagnetic inclusions in the ferromagnetic matrix, can be estimated using the Kersten's expression [8]

$$H_C = p \frac{K_{\text{eff}}}{M_s} \beta^n, \quad (1)$$

where  $p \propto 1/d$ ,  $\beta$  is the inclusion concentration,  $M_s$  is the saturation magnetization,  $K_{\text{eff}}$  is the effective anisotropy constant, and  $n$  is the exponent taking positive values. The nucleation critical field corresponding to the magnetization reversal of the entire sample was determined by Dering [9]

$$H_s = H_0 + \frac{\gamma}{M_s d}, \quad (2)$$

where  $\gamma$  is the DW energy,  $d$  is the grain size, and  $H_0$  is the additional field related to the potential barriers, which prevent the DW motion.

Both investigated mechanisms that cause the magnetic hysteresis upon magnetization reversal in the films under study can underlie the coercivity growth with increasing solution acidity at small pH values, since the increase in the phosphorous concentration is accompanied by the growth of the number of nonmagnetic inclusions and a decrease in the Co ferromagnetic grain size.

The anomalous decrease in  $H_C$  at the transition of the film from the submicrocrystalline to nanocrystalline state at  $\text{pH} > 8.5$  has apparently the same ori-

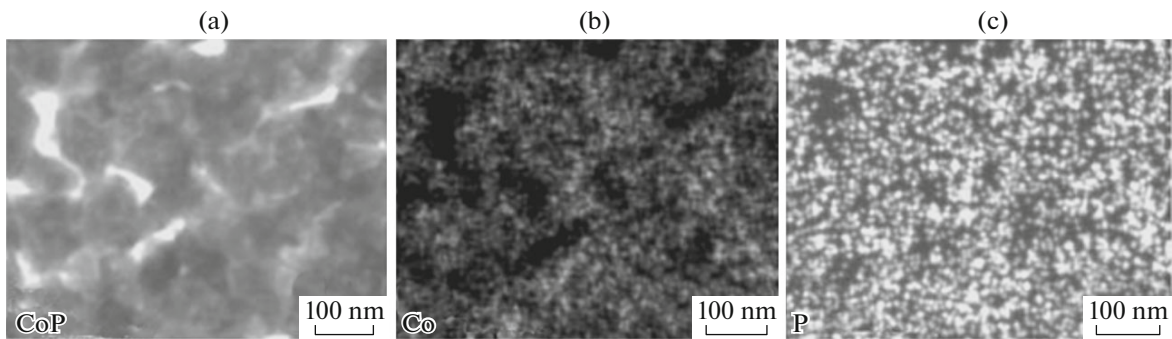


**Fig. 4.** (a) STEM image of the submicrocrystalline CoP film and (b) Co and (c) P distribution maps.

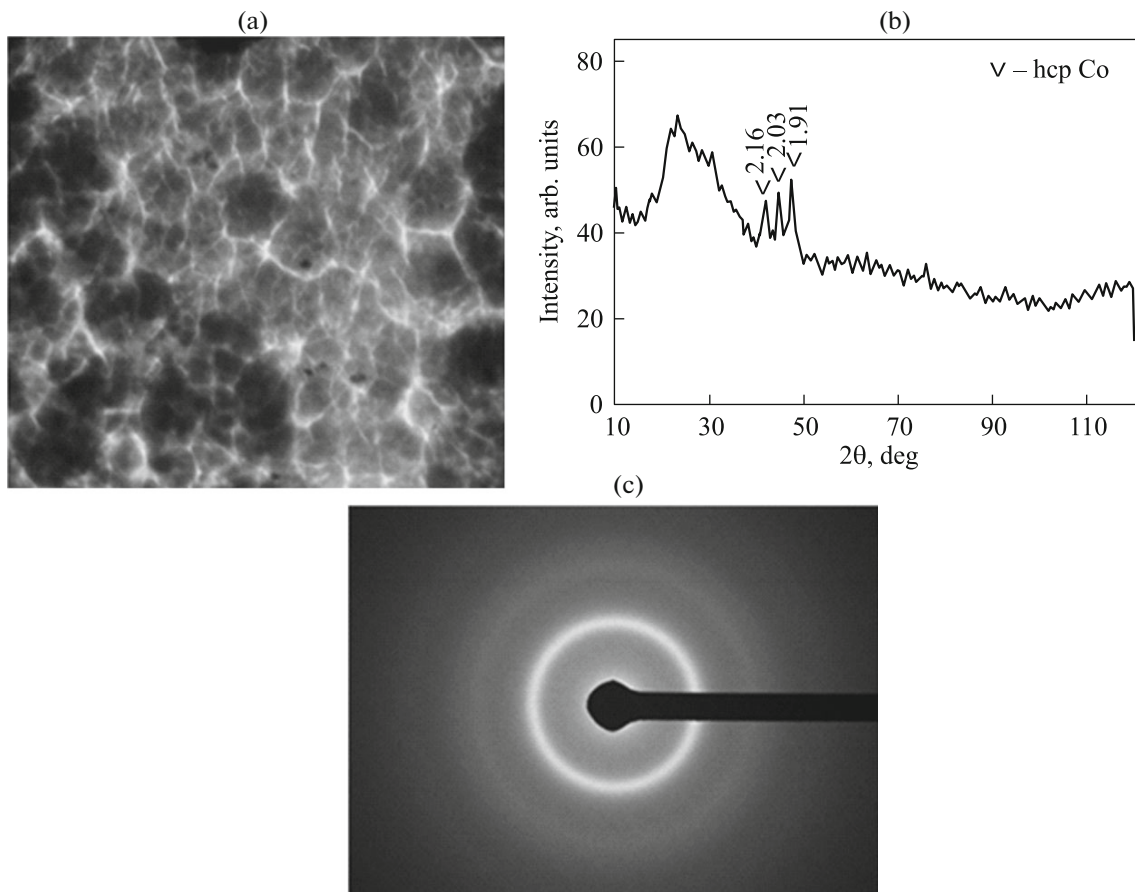


**Fig. 5.** (a) STEM image, (b) X-ray diffraction pattern, and (c) electron diffraction pattern of the nanocrystalline CoP film. Digits above the peaks indicate interplane distances (Å) in the Co crystal lattice.

gin as in the nanocrystalline magnetically soft alloys with the granular structure [10]. If the grain size becomes smaller than the critical value  $d_c$ , the significant role in the materials is played by the volume energy, which decreases the contribution of the magnetic anisotropy of randomly oriented grains to the

total energy. The  $d_c$  value is determined by the balance of these two energies and is similar to the DW width in a ferromagnet

$$L_0 = \sqrt{\frac{A}{K_1}}, \quad (3)$$

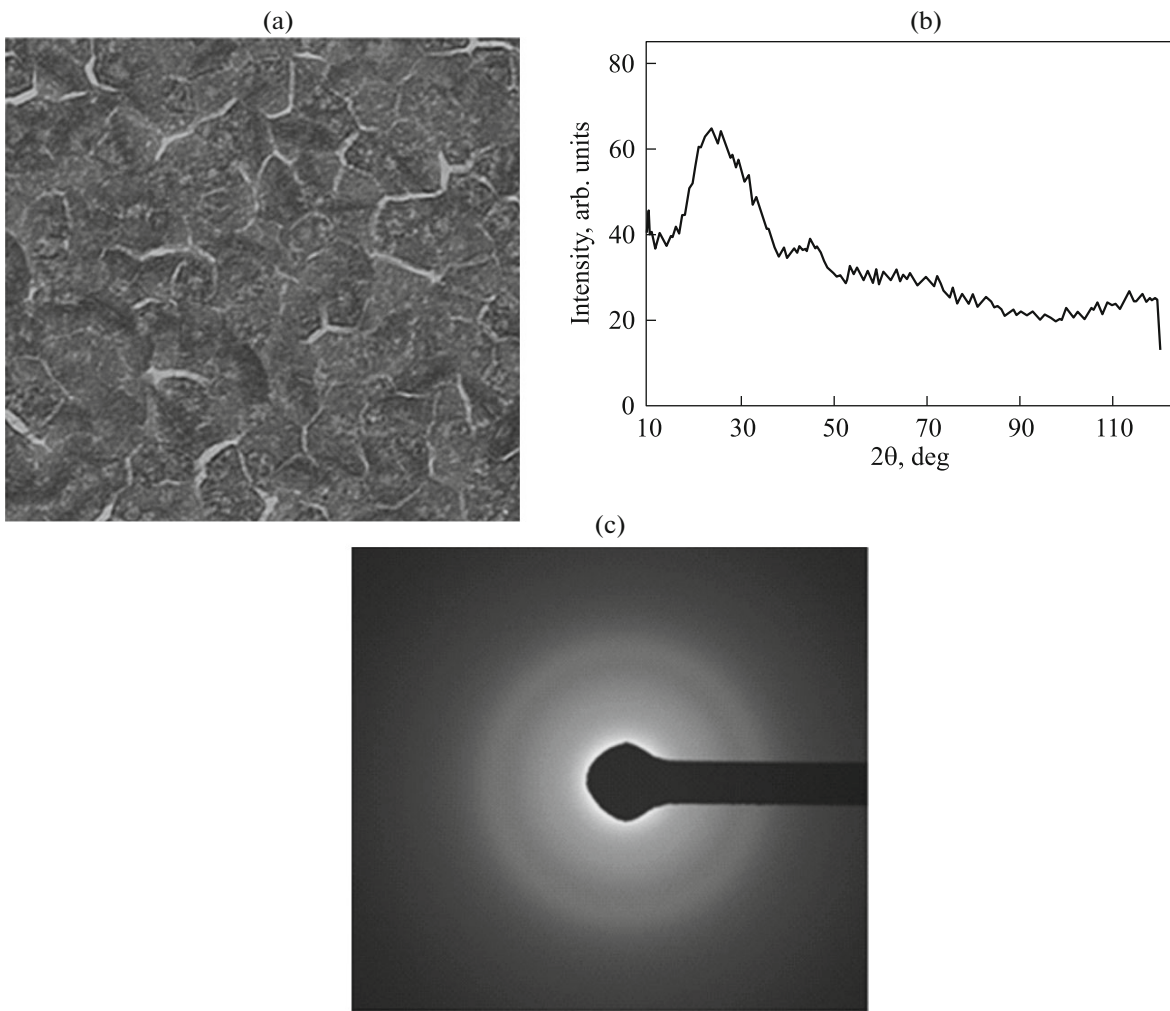


**Fig. 6.** (a) STEM image, (b) X-ray diffraction pattern, and (c) electron diffraction pattern of the amorphous CoP film.

where  $A$  is the exchange constant and  $K_1$  is the anisotropy constant.

Since for the CoP films we have  $K_1 = 4.3 \times 10^5 \text{ J/m}^3$  (hcp Co [11]) and  $A \sim 10^{-11} \text{ J/m}$  (CoP alloy [12]), from (3) we find a critical grain size of  $\sim 4.8 \text{ nm}$ , which corresponds to the crystallite size in the transition region.

## 5. CONCLUSIONS

Based on the data obtained, we can draw the following conclusions. In the low acidity region with  $\text{pH} < 8.5$ , the CoP films consist of submicrocrystalline grains with the hcp lattice. At this solution acidity, the coercivity grows due to an increase in the number of nonmagnetic inclusions and a decrease in the grain size. The coercivity drop at  $\text{pH} > 8.5$  is related to a sharp decrease in the effective anisotropy at the transition of the film from the submicrocrystalline to nanocrystalline state. In addition, we can conclude that the CoP films obtained at  $\text{pH} \sim 8.5$

have the properties typical of compact nanocrystalline materials.

## ACKNOWLEDGMENTS

The authors thank G.V. Bondarenko for help in X-ray diffraction investigations.

This study was supported in part by the Russian Foundation for Basic Research, project no. 14-02-00238-a.

## REFERENCES

1. V. V. Bondar<sup>2</sup>, in *Electrochemistry-1966, Achievements of the Science* (VINITI, Moscow, 1968), p. 56 [in Russian].
2. A. V. Chzhan, T. N. Patrusheva, S. A. Podorzhyak, V. A. Seredkin, and G. N. Bondarenko, *Bull. Russ. Acad. Sci.: Phys.* **80**, 692 (2016).

3. A. Brenner and G. Riddell, *J. Res. Natl. Bur. Stand.* **39**, 385 (1947).
4. O. M. Glenn and B. H. Juan, *Electroless Plating: Fundamentals and Applications* (Orlando, 1990).
5. A. V. Chzhan, G. S. Patrin, S. Ya. Kiparisov, V. A. Seredkin, and M. G. Pal'chik, *Phys. Met. Metallogr.* **109**, 611 (2010).
6. T. A. Tochitskii and L. V. Nemtsevich, *Russ. J. Electrochem.* **34**, 857 (1998).
7. N. Lu, J. Cai, and L. Li, *Surf. Coat. Technol.* **206**, 4822 (2012).
8. M. Kersten, *Z. Phys.* **124**, 714 (1948).
9. V. Dering, *Usp. Fiz. Nauk* **22**, 78 (1939).
10. G. Herzer, in *Handbook of Magnetic Materials*, Ed. by K. H. J. Buchow (Elsevier Science B.V., Amsterdam, 1997), p. 415.
11. S. V. Vonsovsky, *Magnetism* (Nauka, Moscow, 1971; Wiley, Chichester, 1974).
12. R. S. Iskhakov and R. G. Khlebopros, KIPh Preprint (Kirenskii Inst. Phys. Siberian Branch of Acad. Sci. USSR, Krasnoyarsk, 1980).

*Translated by E. Bondareva*